European Polymer Journal 244 (2026) 114509

Contents lists available at ScienceDirect

European Polymer Journal

journal homepage: www.elsevier.com/locate/europolj

Fabrication of single-chain polymer nanoparticles by light-induced inverse electron demand diels-alder (Photo-IEDDA) reaction

Adalet Nur Altunkaya [a,1], Binnur Aydogan Temel [b], Muhammet U. Kahveci [c,*]

[a] Istanbul Technical University, Graduate School, Chemistry Programme, Maslak, Sariyer 34467 Istanbul, Türkiye
[b] Bezmialem Vakif University, Faculty of Pharmacy, Department of Pharmaceutical Chemistry, Fatih, 34093 Istanbul, Türkiye
[c] Istanbul Technical University, Faculty of Science and Letters, Department of Chemistry, Maslak, Sariyer 34467 Istanbul, Türkiye

ARTICLE INFO

Keywords:
Single-chain polymer nanoparticles
Chain folding
IEDDA
Photochemistry
Light-induced click

ABSTRACT

Single-chain polymer nanoparticles (SCNPs) have garnered significant attention due to their ability to mimic the folding behavior of proteins and their potential in applications such as drug delivery, catalysis, and sensing. Herein, we present a novel approach for preparation of SCNPs using a photo-induced inverse electron-demand Diels-Alder (photo-IEDDA) reaction. The base polymer, P(MMA-*co*-HEMA), synthesized *via* reversible addition-fragmentation chain transfer (RAFT) polymerization, was functionalized with dihydrotetrazine (dHTz) and norbornene (Nb) moieties through esterification over HEMA units. Upon irradiation of a dilute solution of the modified polymer, P(MMA-*co*-HEMA)-*M*−PPA−dHTz/Nb, in the presence of a photosensitizer, dihydrotetrazine groups were *in situ* converted to reactive tetrazine moieties, enabling intramolecular crosslinking *via* the photo-IEDDA reaction. This process yielded sub-10 nm SCNPs with high precision and control. The integration of light-triggered reactivity with efficient click chemistry highlights the potential of this method for the scalable production of well-defined SCNPs with tailored properties for advanced applications in nanotechnology and materials science.

1. Introduction

Single-chain polymer nanoparticles (SCNPs) are well-defined polymer nanoparticles that mimic the organization and folding of proteins [1,2]. SCNPs refer to nanoscale structures that arise from the unique folding of a single polymer chain through cross-linking. A fundamental characteristic of SCNPs is their large surface-to-volume ratio, attributed to their small size. This feature makes SCNPs prominent materials in various applications, including chemical catalysis [3,4], sensors [5–7], and drug delivery [8,9].

The folding of SCNPs depends on the intramolecular physical interactions that are also observed in protein folding. However, in polymer folding, diverse covalent, dynamic covalent, and non-covalent cross-linking methods are employed [10–12]. These include radical coupling [13], photo-induced cycloaddition [14,15], metal ligation [16], *click* chemistry [17], nuecleophilic substitution [18,19], Michael Addition reactions [20–22], and supramolecular interactions [23,24]. Among these reactions, *click* chemistry offers several advantages, such as forming covalent bonds efficiently under mild conditions without generating by-products.

A notable example of the click reactions is inverse electron-demand Diels-Alder (IEDDA) reaction, a [4 + 2] cycloaddion between an electron-rich dienophile and an electron-poor conjugate diene, namely tetrazine. Due to its bioorthogonal nature, fast kinetics, and high efficiency, the IEDDA reaction has been extensively used in various bio-applications [25–27] and material chemistry [28,29]. O'Reilly and coworkers employed this reaction in the preparation of SCNPs [30]. In their study, polymers bearing norbornene moieties as side chains were collapsed and crosslinked using a bis-tetrazine functional crosslinker. Since tetrazines are highly reactive and react immediately with norbornene, the biz-tetrazine crosslinker was added slowly to a dilute solution of norbornene-functional polymer. Remote control over the initiation of such reactions can provide significant advantages, such as achieving high yields and selectivity. Light-induced click reactions combine the benefits of both click chemistry and light-trigered processes [31]. For example, the temporal and spatial control of click reactions enables the fabrication of well-defined and well-controlled materials in high yields and selectivity [32]. Recently, a photo-induced inverse

* Corresponding author.
E-mail address: kahvecimuh@itu.edu.tr (M.U. Kahveci).
[1] Current address at: Istanbul University, Faculty of Science, Department of Chemistry, Vezneciler, 34134 Istanbul, Türkiye.

https://doi.org/10.1016/j.eurpolymj.2026.114509
Received 26 September 2025; Received in revised form 26 December 2025; Accepted 7 January 2026
Available online 16 January 2026

electron-demand Diels-Alder (photo-IEDDA) reaction has been developed by our group and others [33–35]. In this reaction, dihydrotetrazine (dHTz) molecules, which are initially inactive in IEDDA reaction, can be photochemically converted to active tetrazine (Tz) molecules upon irradiation in the presene of a photosensitizer.

Herein, a novel approach utilizing the photo-IEDDA reaction for the fabrication of intramolecularly crosslinked SCNPs was developed. Firstly, P(MMA-*co*-HEMA) was synthesized by reversible addition-fragmentation chain transfer (RAFT) polymerization and modified with 4-oxo-4-((6-(6-(pyridin-2-yl)-1,2,4,5-tetrazin-3-yl)pyridin-3yl) amino) butanoic acid (PPA-dHTz-COOH) and an acid derivative of norbornene (Nb) through esterification. The resulting modified polymer, P(MMA-*co*-HEMA)-*M*−PPA−dHTz/Nb, was subsequently employed for SCNP formation *via* a photo-IEDDA reaction. In this process, dihydrotetrazine groups on the polymer were *in situ* converted into reactive tetrazine moieties by irradiating a dilute polymer solution in the presence of a photosensitizer. The irradition successfully induced crosslinking, resulting in the formation of polymer nanoparticles with sub-10 nm sizes.

2. Experimental section

2.1. Materials

5-Amino-2-pyridine carbonitrile (Sigma-Aldrich, 96 %), 2-pyridine carbonitrile (Sigma, 99 %), hydrazine monohydrate (Sigma-Aldrich, 98 %), succinic anhydride (Sigma-Aldrich), methyl methacrylate (MMA) (Sigma, 99 %), 2-hydroxyethyl methacrylate (HEMA) (Sigma Aldrich, 98 %), azobisisobutyronitrile (AIBN) (Sigma Aldrich, 98 %), 4-cyano-4-[(dodecylthiosulfanylthiocarbonyl) sulfanyl]pentanoic acid (CTA) (97 %, HPLC, Sigma Aldrich), bicyclo[2.2.1]hept-5-ene-2-carboxylic acid (norbornene carboxylic acid) (95 %, Oxchem), *N*,*N*'-1,3-dicyclohexylcarbodiimide (DCC) (Aldrich), 4-(dimethylamino)pyridine (DMAP) (Sigma, >98 %), methylene blue (Sigma-Aldrich), and other chemicals were used as purchased. Tetrahydrofuran (THF) (Merck) was refluxed over metallic sodium and dried before use.

2.2. Instrumentation

An Agilent VNMRS 500 Nuclear Magnetic Resonance (NMR) spectrometer was used for ^{1}H NMR analyses at room temperature in deuterated solvents with $Si(CH_3)_4$ as an internal standard. UV–Vis spectroscopy analyses were performed on a Peak Instruments C-7000UV spectrophotometer with 1 cm path length cuvette. Fourier Transform Infrared (FT-IR) spectra were recorded on an Agilent Technologies Cary 630 FT-IR instrument. Photooxidation of dihydrotetrazines was carried out with a red laser (CNI Laser, Model No: FC-680–2 W; $\lambda \sim 680$ nm). Molecular masses of the polymers were determined by size exclusion chromatography (SEC) instrument, Viscotek GPCmax Autosampler system consisting of a pump, three ViscoGEL columns (G2000HHR, G3000HHR, and G4000HHR), and a Viscotek differential refractive index detector. Tetrahydrofuran was used as the eluent at a flow rate of 1.0 mL min^{-1}. Number average molecular masses were determined using linear polystyrene standards. Differential Scanning Calorimetry (DSC) measurements were performed on a TA Instruments Discovery DSC 250 with a heating rate rate of 10 °C min^{-1} under nitrogen atmosphere. Particle size distributions were determined using dynamic light scattering (DLS) in THF dispersions using a Malvern NanoZSP instrument. Single-chain polymer nanoparticles (SCNPs) were imaged on a Thermo Scientific Quattro ESEM scanning electron microscope using a scanning transmission electron microscopy (STEM) detector under high vacuum (30 kV) and the digital images of SCNPs were captured to analyze their morphology.

2.3. Synthesis of 6-(6-(pyridin-2-yl)-1,4-dihydro-1,2,4,5-tetrazin-3-yl) pyridin-3-amine (PPA-dHTz)

2-Pyridinecarbonitrile (2.00 g, 19.2 mmol, 1 eq.), 5-amino-2-pyridinecarbonitrile (1.14 g, 9.6 mmol, 0.5 eq.), and sulphur (0.60 g) were dissolved in ethanol (9 mL) under nitrogen gas purge. Hydrazine monohydrate (5 mL, 103.2 mmol, 5.4 eq.) was added dropwise with the aid of a syringe to the flask in an ice bath (0 °C). The reaction mixture was stirred at room temperature for 2 h. Then, the color changed to orange, and the reaction mixture was heated to 90 °C and refluxed for 2 h. After two hours, the reaction mixture was brought back to room temperature and stirred overnight. Subsequently, the mixture was cooled to 0 °C and the solid crude product was filtered, washed with cold ethanol (3 x 15 mL), and dried under vacuum. The crude product (PPA-dHTz) was purified by column chromatography (chloroform/ethanol, 15/1) (998 mg, 41 % yield) [36].

^{1}H NMR (500 MHz, DMSO-d_6, δ (ppm)) 8.70 (s, 1H), 8.64 (s, 1H), 8.62 (s, 1H), 7.95 (d, 1H), 7.92 (d, 2H), 7.65 (d, 1H), 7.50 (s, 1H), 6.99 (dd, 1H), 5.87 (s, 2H).

2.4. Synthesis of 4-oxo-4-((6-(6-(pyridin-2-yl)-1,4-dihydro-1,2,4,5-tetrazin-3-yl) pyridin-3-yl) amino) butanoic acid (PPA-dHTz-COOH)

PPA-dHTz (200 mg, 0.79 mmol), succinic anhydride (400 mg, 4.00 mmol), and dried THF (8 mL) were added to a Schlenk tube under N_2 atmosphere. The reaction was continued under constant stirring for 24 h at 70 °C. Then, the mixture was cooled in an ice bath. The precipitate was filtered and sequentially washed with THF (2 mL) and ethyl acetate (3x3 mL). The crude product was dried under vacuum (279 mg, yield: >99 %) [37].

^{1}H NMR (500 MHz, DMSO-d_6, δ (ppm)) 12.18 (br, 1H), 10.44 (s, 1H), 8.93 (s, 1H), 8.87 (s, 1H), 8.81 (d, 1H), 8.63 (d, 1H), 8.13 (dd, 1H), 7.95 (m, 3H), 7.52 (ddd, 1H), 2.62 (t, 2H), 2.54 (t, 2H).

^{13}C NMR (100 MHz, DMSO-d_6, δ (ppm)): 174.32, 171.54, 149.04, 147.74, 146.8, 146.53, 141.82, 139.17, 137.84, 137.71, 126.96, 125.75, 121.86, 121.4, 31.58, 29.25.

2.5. Synthesis of poly(methyl metacrylate-co-2-hydroxyethyl methacrylate) [P(MMA-co-HEMA)]

The synthesis of random copolymer poly(methyl metacrylate-*co*-2-hydroxyethyl methacrylate) [P(MMA-*co*-HEMA)] was accomplished by using the ratio of reagents [MMA]:[HEMA]:[CTA]:[AIBN] = 220:95:1:0.3. MMA (2.5 mL, 23.4 × 10^{-3} mol), HEMA (1.22 mL, 10.1 × 10^{-3} mol) and CTA (43 mg, 1.06 × 10^{-4} mol) were dissolved in dried THF (14 mL) in a Schlenk tube. After addition of AIBN (5.2 mg, 3.2 × 10^{-5} mol), the reaction tube was closed and tightly sealed. Then the reaction solution was degassed by three cycles of freeze-vacuum-thaw and the tube was saturated with nitrogen gas. The tube was immersed in a preheated (70 °C) silicon oil and the reaction solution was stirred continuously at 70 °C overnight. Aftewards, the tube content was cooled and exposed to air to quench the polymerization. The resultant polymer was precipitated twice in diethyl ether. Light-yellow polymer was filtered. The pure polymer had a gravimetric monomer conversion rate of 48 % and theoritical molecular mass of 16,550 g/mol. Molecular mass was determined as M_n = 19,980 g/mol (M_w/M_n = 1.32) by SEC (eluent THF) (Scheme S3) [38].

2.6. Synthesis of P(MMA-co-HEMA)-M−PPA−dHTz

Dihydrotetrazine side groups were introduced onto the polymeric backbones by esterification reaction between the hydroxyl groups on P(MMA-*co*-HEMA) and PPA-dHTz-COOH (Scheme S4). In a 50 mL two-necked flask under a nitrogen atmosphere, PPA-dHTz-COOH (73 mg, 0.206 mmol) was dissolved in dried THF (7 mL) before the flask was immersed into ice-water bath. Under magnetic stirring, DCC (85 mg, 0.412 mmol) and DMAP (5 mg, 0.041 mmol) in THF (2 mL) was added into the mixture within 5 min at 0 °C. After stirring for two hours, P(MMA-*co*-HEMA) (150 mg, 7.51×10^{-6} mol) in THF (5 mL) was added into the mixture. The reaction continued overnight in a 50 °C oil bath. The solvent was concentrated using a rotatory evaporator and was precipitated in water and hexane sequentially. The modified polymer was obtained as dark yellow/brown solid by centrifugation and dried under vacuum overnight.

2.7. Synthesis of P(MMA-co-HEMA)-M−PPA−dHTz/Nb

In a 50-mL two-necked flask under a nitrogen atmosphere, Nb-COOH (28.5 mg, 0.206 mmol) was dissolved in dried THF (5 mL) before the flask was immersed into ice-water bath. Under magnetic stirring, DCC (85.2 mg, 0.413 mmol) and DMAP (5.1 mg, 0.042 mmol) in THF (2 mL) was added into the mixture within 5 min at 0 °C. After stirring for two hours, P(MMA-*co*-HEMA)-PPA-dHTz (150 mg) in THF (10 mL) was added into the mixture (Scheme S5). The reaction was continued overnight in a 50 °C oil bath. The solvent was concentrated using a rotatory evaporator and the modified polymer was precipitated in hexane. The crude product was obtained by centrifugation and dried under vacuum overnight.

2.8. Photooxidation reaction of PPA-dHTz-COOH

The photooxidation reaction of the PPA-dHTz-COOH molecule was carried out using a red laser (λ: 680 nm, light intensity: 60 %, light intesnsity: 0.3 W/cm^2). Initially, a solution containing PPA-dHTz-COOH (21 μM) and methylene blue (8 μM) in ethanol was prepared. This solution was placed in a UV cuvette and irradiated with the red laser to induce the oxidation of PPA-dHTz-COOH to PPA-Tz-COOH. The progress of this oxidation reaction was monitored at specific intervals by recording absorbance values at 290 and 325 nm [37].

2.9. Preparation of single-chain polymer nanoparticles (SCNPs)

P(MMA-*co*-HEMA)-*M*−PPA−dHTz/Nb (50 mg) was dissolved in ethanol (100 mL or 250 mL) containing Methylene Blue (8 μM). Subsequently, the solution was irradiated using a red laser (λ: 680 nm, light intensity: 60 %, light intensisty: 0.3 W/cm^2) for 2 h at room temperature (~25 °C), and the oxidation of the dihydrotetrazine moiety on the polymer was monitored with UV–Vis spectroscopy. At the end of the irradiation period, the reaction mixture was stirred overnight in the dark at room temperature (~25 °C) or 80 °C to assure accomplishment of the IEDDA reaction. After that, the solution was concentrated by evaporating excess solvent and the resultant SCNP was precipitated in water. Finally, the SCNP was filtered, washed three times with water, and dried under vacuum. Three different conditions were used in SCNP formation (see Table 2).

3. Results and discusion

A novel approach relying on light-induced inverse electron demand Diels-Alder (photo-IEDDA) reaction was developed for the preparation of SCNPs. Principally, a dihydrotetrazine molecule is oxidized photochemically *in situ* yielding a tetrazine molecule which subsequently undergoes IEDDA reaction with a partner molecule such as norbornene [34] and *trans*-cyclooctenes [33,37,39]. In the current work, this light-induced rapid and efficient reaction was adopted for fabrication of SCNPs utilizing a single polymer chain bearing both dihydrotetrazine and its partner molecule, norbornene. The precursor dihydrotetrazine with a carboxylic acid functionality (PPA-dHTz-COOH) was prepared over two steps. Firstly, PPA-dHTz was synthesized by following previous reports, and then reacted with succinic anhydride to get a caboxylic acid handle [37]. The ^{1}H NMR spectra of PPA-dHTz and PPA-dHTz-COOH given in Fig. S1 and S2 exhibit all typical peaks and support the synthesis of the corresponding molecules. The aromatic peaks at 8.62, 7.96–7.88, 7.64, 7.51 and 6.98 ppm perfectly fit the structure of the PPA-dHTz. Proton peaks ascribed to the secondary and the terminal amine were observed at 8.89 and 8.64 ppm, and 5.87 ppm, respectively. In addition to corresponding aromatic and secondary amine peaks, new aliphatic peaks (2.55–2.70 ppm) atributed to succinic acid moiety appeared in the ^{1}H NMR spectrum of PPA-dHTz-COOH (Fig. S2). In addition, primary amine proton peaks disapperead and a new secondary amine proton peak and carboxylic acid proton peak were observed at 10.44 ppm and 12.20 ppm, repectively. ^{13}C NMR spectrum of PPA-dHTz-COOH (Fig. S3) also confirms the structure since the peak corresponding to the amide carbonyl carbon at 174 ppm and the peak corresponding to the carboxylic acid carbonyl carbon at 171 ppm fit the structure perfectly.

The precursor polymer, P(MMA-*co*-HEMA), was synthesized via RAFT polymerization and chemical structure of the polymer was confirmed by ^{1}H NMR spectroscopy (Fig. S4). While peaks corresponding to protons of the methyl ester of the MMA unit are observed at 3.66 ppm (peak c), protons of the methylene groups adjacent to the hydroxyl (–OH) group in the HEMA unit were observed at 3.85 (peak b) and 4.12 ppm (peak a). The ratio of the integral areas of peaks “a” and “b” to the integral area of peak “c” was used to determine the copolymerization ratio of MMA and HEMA units. The number of repeating units was determined using the gravimetric conversion and NMR data, and using SEC and NMR data (Table 1). The molecular mass of P(MMA-*co*-HEMA) was determined to be 19,980 g/mol ($M_{n,SEC}$) with a PDI of 1.32 by SEC analysis (with THF as the eluent). On the other hand, the theoretical molecular mass ($M_{n,theoretical}$) was calculated as 16,550 g/mol.

P(MMA-*co*-HEMA) was then modified with PPA-dHTz-COOH and norbornene carboxylic acid (Nb-COOH) via esterification over hydroxyl groups of the HEMA units in sequential two post-polymerization modifications. After the modification with PPA-dHTz-COOH, the NMR spectrum of the polymer, P(MMA-*co*-HEMA)-dHTz, exhibited typical proton peaks of the dihydrotetrazine groups in the range of 6.98–8.70 ppm. In addition, distinguishable signals due to methylene protons of succinyl ester which were observed at 2.85 ppm and 2.82 ppm allowed

Table 1
Molecular mass and repating units of P(MMA-*co*-HEMA).

Polymer	Number of MMA unit			Number of HEMA unit			$M_{n,theoretical}$(kDa)	$M_{n,SEC}$(kDa)	$M_{w,SEC}$(kDa)	PDI *
	feed	by NMR and conversion	by SEC and NMR	feed	by NMR and conversion	by SEC and NMR				
P(MMA-*co*-HEMA)	220	105.6	127	95	66.5	55	16.55	19.98	26.40	1.32

* Polydispersity index (PDI) (M_w/M_n) was obtained from SEC analysis.

Table 2
Properties of the precursor polymer and the resultant SCNPs. The SCNPs were obtained by irradiation with a red laser (λ: 680 nm, light intensisty: 0.3 W/cm^2) for 2 h at room temperature (~25 °C) followed by stirring overnight at room temperature (~25 °C) or 80 ℃ stirring in the dark.

Polymeric Nanoparticle	Post-irradiation temperature (℃)[a]	*C* (mg/mL)[b]	M_n (g/mol)[c]	PDI[c]
Precursor polymer	–	–	20,130	1.54
SCNP-1	25	0.5	18,880	1.73
SCNP-2	80	0.5	14,050	1.42
SCNP-3	80	0.2	13,920	1.44

[a] In all cases, irradiations were performed at 25 ℃. After irradition, the dark reactions were conducted at the specified temperature.
[b] Concentration of the preccursor polymers used in SCNP formation.
[c] Molecular mass (M_n) and polydispersity index (PDI) were determined by SEC.

calculation of functionalization efficiency. On the basis of NMR calculations, 27 mol% of hydroxyl groups of HEMA units were converted into dihydrotetrazine groups after the postmodification.

In the second step, Nb-COOH was grafted to P(MMA-*co*-HEMA)-*M*−PPA−dHTz via esterification between Nb-COOH and the remaining hydroxyl groups of the HEMA units. In addition to all other proton signals observed in the NMR spectrum of P(MMA-*co*-HEMA)-*M*−PPA−dHTz, typical norbornene olefinic proton peaks appeared around 5.92–6.22 ppm supporting successful grafting of the norbornene functionalities in the NMR spectrum of P(MMA-*co*-HEMA)-*M*−PPA−dHTz/Nb (Fig. 1). Based on the NMR calculations, the conversions of hydroxyl groups to Nb and dHTz were determined to be 35.8 mol% and 23.4 mol%, respectively. Accordingly, approximately 19.7 and 12.9 of the 55 HEMA units were conjugated with Nb and dHTz groups, respectively.

The chemical structures of the polymers and PPA-dHTz-COOH were also confirmed by FT-IR spectroscopy as shown in Fig. 2. The band at 3302 and 1677 cm^{-1} were perfectly attributed to amine and amide carbonyl groups of PPA-dHTz-COOH, respectively. In addition, broad band observed from 3400 to 2000 cm^{-1} was ascribed to carboxylic acid of PPA-dHTz-COOH. P(MMA-*co*-HEMA)-*M*−PPA−dHTz and P(MMA-*co*-HEMA)-*M*−PPA−dHTz/Nb exhibited bands around 3500 cm^{-1} and 3300 cm^{-1} due to amines of dihydrotetrazine groups and hydroxyl groups of the HEMA units, correspondingly. The carbonyl stretching band of amide and ester groups of the polymers were observed at 1677 cm^{-1} and 1726 cm^{-1}, respectively.

Dihydrotetrazines are unreactive against olefins, but 1,2,4,5-tetrazines readily undergo IEDDA reaction with certain olefins such as *trans*-cyclooctene and norbornene [33,35]. This feature allows preparation of polymers containing both norbornene and dihydrotetrazine groups at the same time. In the current approach, the dihydrotetrazine groups are photochemically oxidized *in situ* to form tetrazines, which subsequently undergo an IEDDA reaction with norbornenes on the same polymer chain. A model reaction was designed to monitor the photochemical oxidation of PPA-dHTz-COOH prior to its implementation in SCNP fabrication. Photooxidation was monitored using UV–Vis spectroscopy upon irradiation of PPA-dHTz-COOH (21 μM) with a red laser (laser (λ: 680 nm, laser power: 60 %, light intensity: 0.3 W/cm^2) in the presence of a photosensitizer, namely Methylene Blue (8 μM), in ethanol. Upon irradiation, the absorbance band of dihydrotetrazine at 290 nm decreased, while a new band at 325 nm, attributed to the formation of tetrazine, appeared (Fig. 3-A) [35]. Change in the ratio of the absorbances at these wavelengths (A_{290}/A_{325}) indicates that the photooxidation of dihydrotetrazine to tetrazine occurred very rapidly, within almost 70 s (Fig. 3-B). This rapid photochemical conversion was also reported previously by our group and others [33–35,39].

P(MMA-*co*-HEMA)-*M*−PPA−dHTz/Nb was utilized in SCNP formation through light-induced IEDDA (photo-IEDDA) reaction (Fig. 4). The

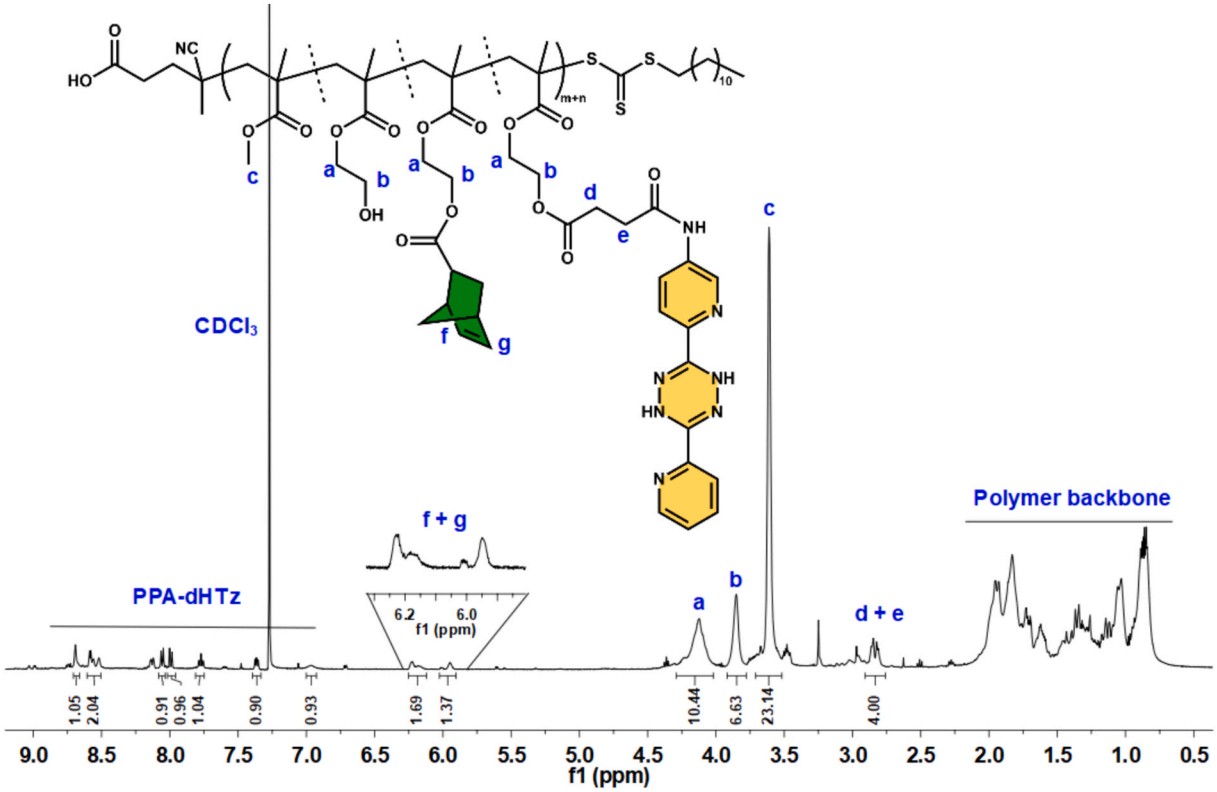

Fig. 1. ^{1}H NMR spectrum of P(MMA-*co*-HEMA)-*M*−PPA−dHTz/Nb ($CDCl_3$).

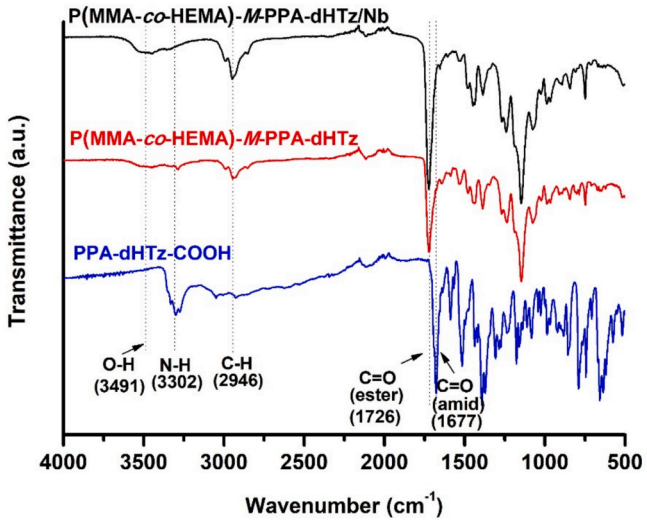

Fig. 2. FT-IR sepectra of PPA-dHTz-COOH, P(MMA-*co*-HEMA)-*M*−PPA−dHTz and P(MMA-*co*-HEMA)-*M*−PPA−dHTz/Nb.

in situ oxidation of dihydrotetrazine grafted onto the polymer was induced by a red laser in the presence of Methylene Blue, and monitored with a UV–Vis spectrophotometer. The absorbance band of the polymer-bound dihydrotetrazine observed at 290 nm decreased as a result of oxidation, while a new absorbance band emerged at 325 nm (Fig. 5). The observation of the similar spectral change in the oxidation of the small molecule dihydrotetrazine derivative, PPA-dHTz-COOH (Fig. 3), supports formation of the tetrazine molecule necessary for IEDDA on the polymer chain. The photooxidation of the small molecule dihydrotetrazine (PPA-dHTz-COOH) was completed in approximately 70 s, whereas the polymer-bound dihydrotetrazine required 96 min. To compare the photooxidation kinetics of free dihydrotetrazine (PPA-dHTz) and polymer-bound dihydrotetrazine, first-order decay plots for both substrates were constructed from the spectral data (Figs. S7 and S8). The ratio of the maximum absorbances of dihydrotetrazine (A_{dHTz} @ λ = 290 nm) and tetrazine (A_{Tz} @ λ = 325 nm) was plotted as a function of irradiation time, yielding excellent fits to a first-order decay model. The first-order rate constants were determined to be $k_{PPA\text{-}dHTz}$ = 4.78 min^{-1} and $k_{Polymer\text{-}dHTz}$ = 0.17 min^{-1}. Accordingly, the small-molecule dihydrotetrazine exhibited a 28-fold higher rate constant than the polymer-bound analogue. This markedly faster photochemical oxidation of the small molecule relative to its polymeric counterpart is attributed to steric hindrance imposed by the macromolecular architecture.

The IEDDA reaction between the in-situ-formed tetrazine and the norbornene groups was confirmed. When comparing the ^{1}H NMR spectra of the SCNPs and the precursor polymer as shown in Fig. 6, disappearance of the peaks ascribed to norbornene (5.92–6.22 ppm) clearly supports the IEDDA reaction between *in situ* generated tetrazine moieties and norbornenes. Change in the chemical shifts of the aromatic protons confirms the reaction as we reported this change in a previous study [33].

The crosslinking reactions under dilute conditions (0.2–0.5 mg/mL) yield formation of SCNPs (Table 2) [40]. The molecular masses of the precursor polymer and the SCNPs were determined using gel permeation chromatography (SEC). The molecular masses (M_n) of SCNPs are generally lower compared to the precursor polymer, due to the decrease in hydrodynamic volumes and their compact morphology [13]. The molecular masses and SEC chromatograms of SCNPs obtained from the same precursor polymer under different conditions (SCNP-1 at 25 °C and SCNP-2 at 80 °C) or different polymer concentrations (SCNP-2 at 0.5 mg/mL and SCNP-3 at 0.2 mg/mL) are provided in Fig. 7. As can be seen, all SCNPs had lower M_n values compared to the precursor polymer as a result of intramolecular crosslinking in dilute conditions. It is understood that SCNPs obtained from reactions conducted at a higher temperature (80 °C) had lower molecular mass, thereby indicating more efficient intramolecular crosslinking. On the other hand, the effect of polymer concentration on molecular mass is understood to be minimal.

To get further insight, the particle size analysis of the precursor polymer and SCNPs was performed via dynamic light scattering (DLS) measurements (Fig. 8-A and Fig. S9). The hydrodynamic radii of SCNP-1 and SCNP-2 were determined to be 6.01 nm and 7.37 nm, respectively; while the radii of the corresponding precursor polymers were measured as 7.23 nm and 9.69 nm, respectively. This result reveals that the nanoparticles having a more compact morphology compared to the polymer, supporting the findings obtained from SEC. Although SCNPs exhibited sub-10 nm particle sizes through DLS measurements, scanning/transmission electron microscopy (STEM) images display that

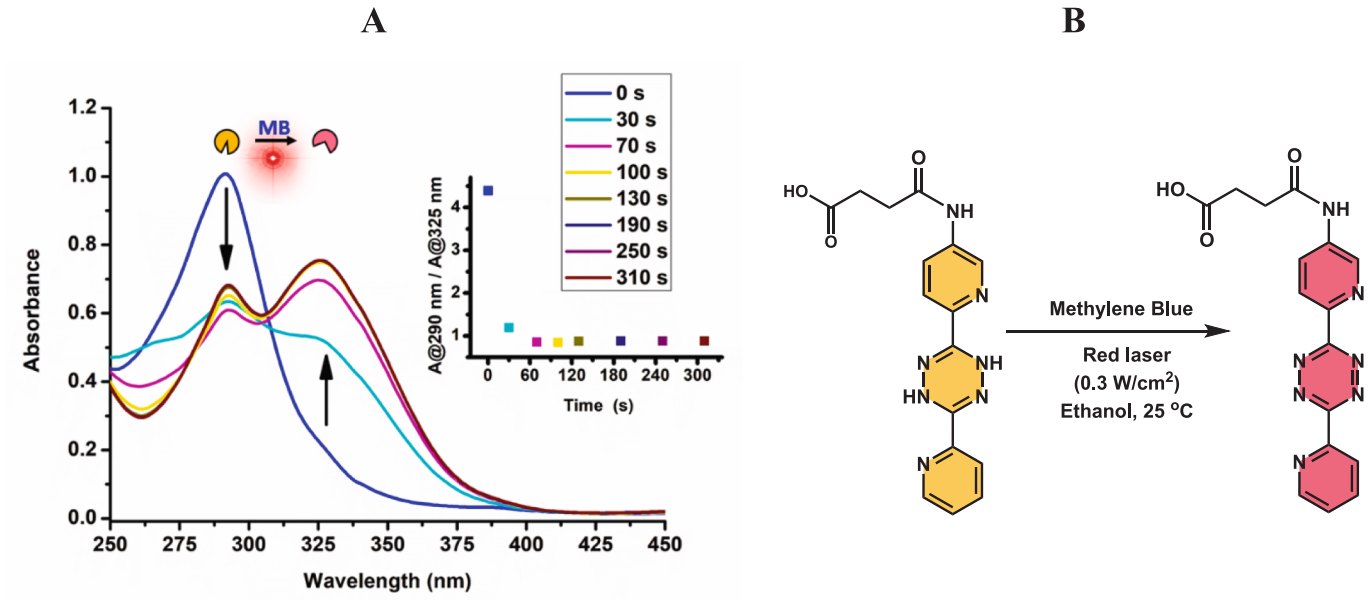

Fig. 3. A) UV–Vis spectral change of a solution containing PPA-dHTz-COOH (21 μM) and Methylene Blue (8 μM), in ethanol upon irradiation with with a red laser (Inset: Change in the ratio of absorbance values at 290 nm and 325 nm). B) Photooxidation of PPA-dHTz-COOH in the preesence of Methylene Blue.

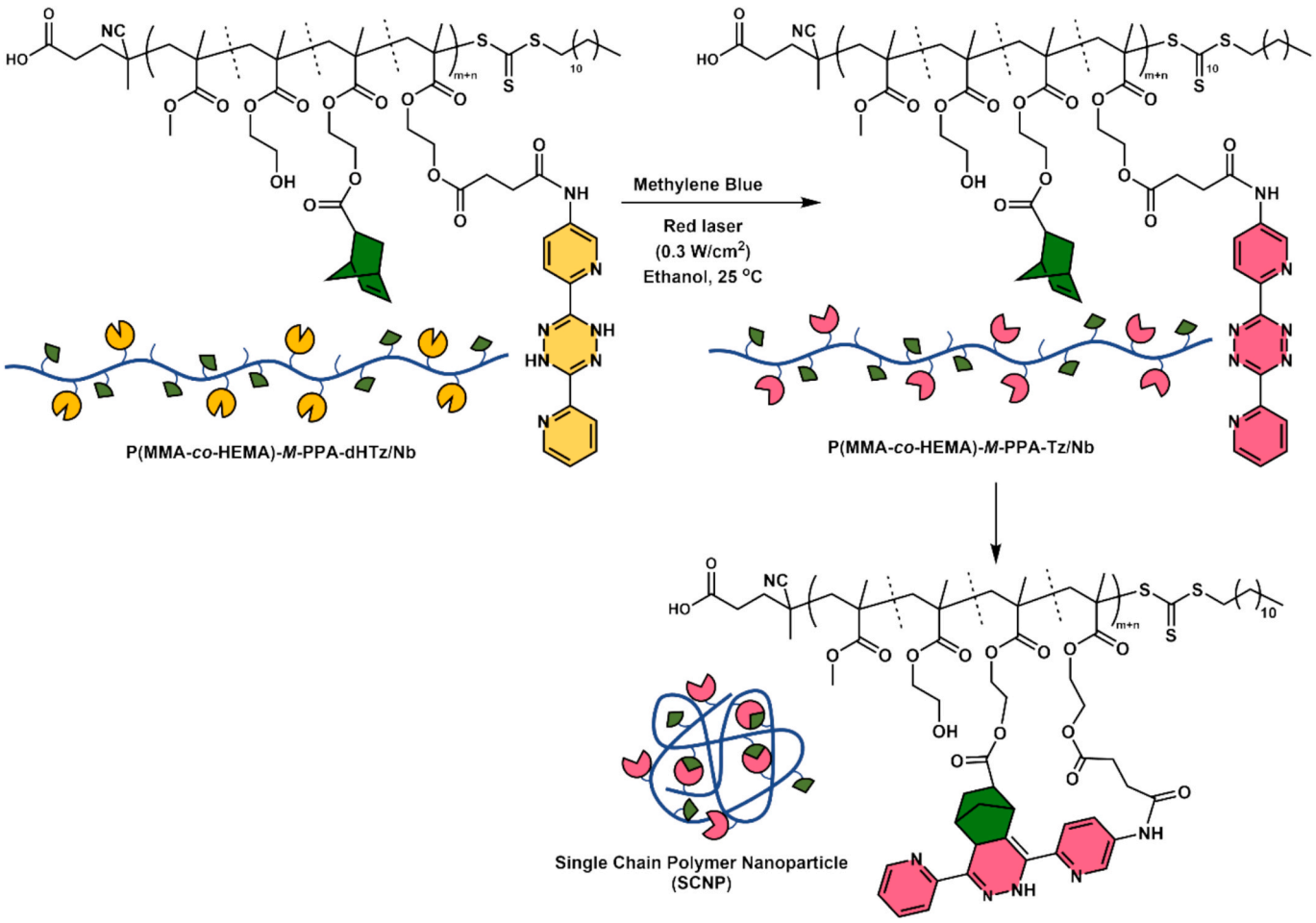

Fig. 4. Formation of SCNP from P(MMA-*co*-HEMA)-*M*−PPA−dHTz/Nb via photo-IEDDA reaction.

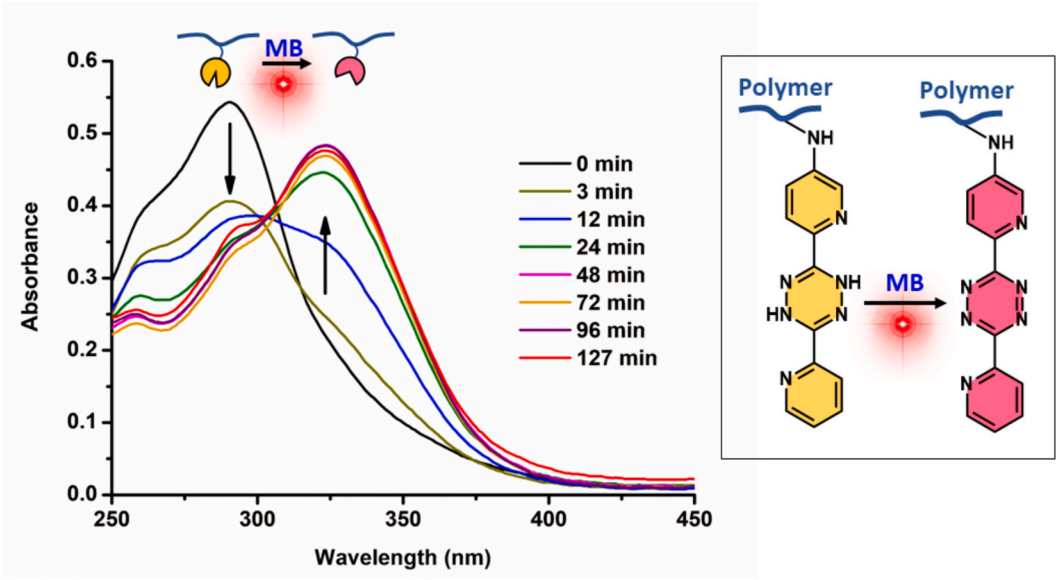

Fig. 5. UV–Vis spectra of the polymer solution during the photooxidation of PPA-dHTz moieties on the polymer induced with a red laser in the presence of Methylene Blue as a photosensitizer.

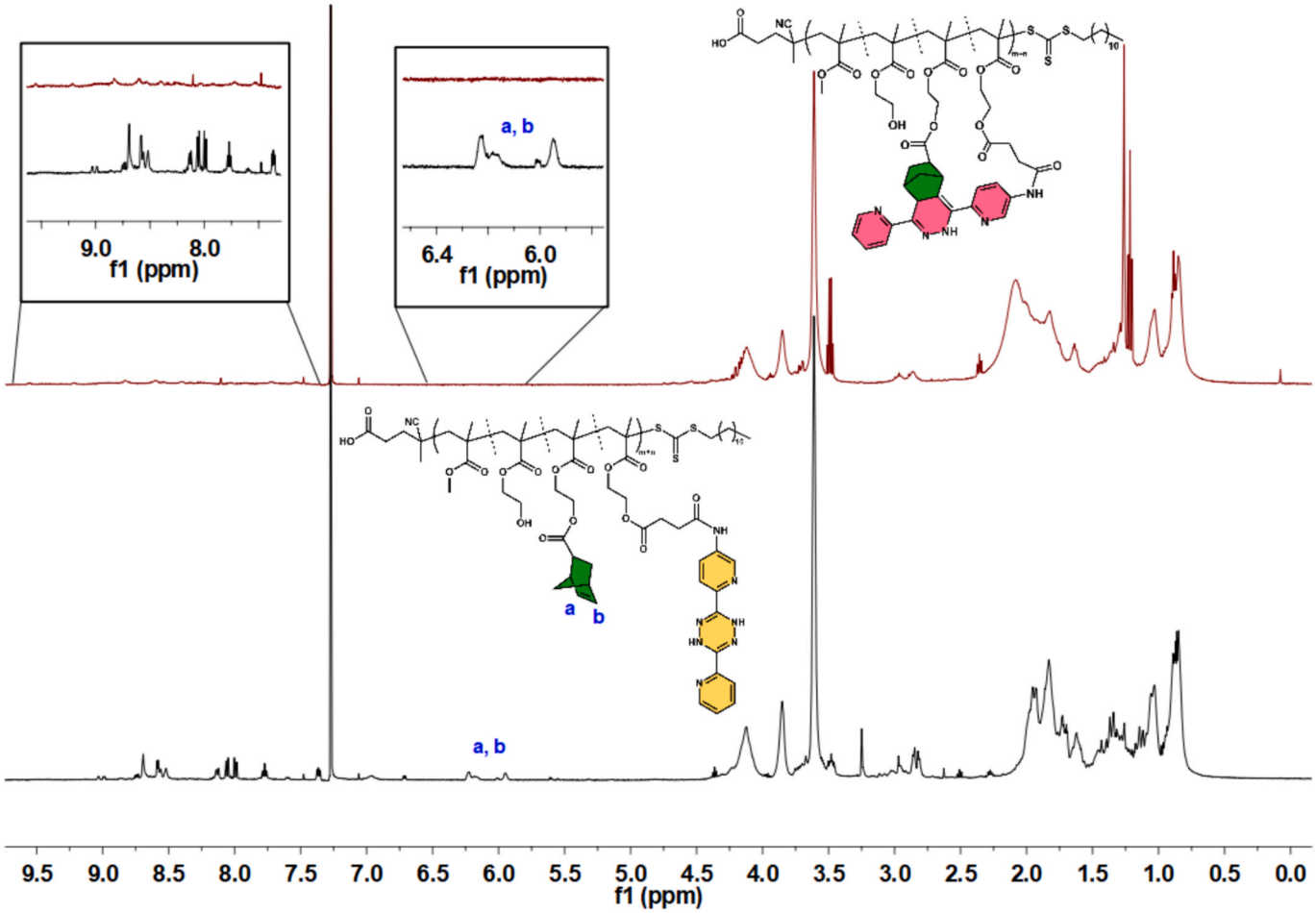

Fig. 6. ^{1}H NMR spectra of SCNP-2 and the precursor polymer.

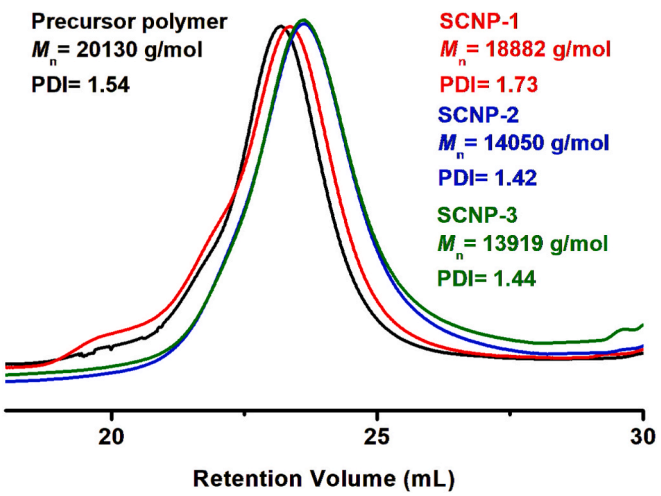

Fig. 7. SEC chromatograms of the precursor polymer and the SCNPs.

SCNPs tend to have larger globular shapes (around 30 nm) (Fig. 8-B). Solvent evaporation after casting on a copper grid might increase chance of intermolecular interactions leading to polymer chain aggregation.

Thermal properties of the precursor polymer and SCNPs were examined by differential scanning calorimetry (DSC) analyses to gain more detailed information. When compared to the precursor polymer, SCNPs showed higher glass transition temperature (T_g) values. T_g of the precursor polymer was observed at approximately 72 °C, while due to the reduction in chain flexibility resulting from intramolecular crosslinking, the T_g values of SCNP-1 and SCNP-2 were determined to be 86 °C and 109 °C, respectively (Fig. 9) [13,41]. Moreover, the higher T_g value of SCNP-2 compared to SCNP-1 can be explained by more effective intramolecular crosslinking in SCNP-2.

Thermal properties of the precursor polymer and SCNPs were examined by differential scanning calorimetry (DSC) analyses to gain more detailed information. When compared to the precursor polymer, SCNPs showed higher glass transition temperature (T_g) values. As shown in Fig. 9, the precursor polymer exhibited a T_g of approximately 72 °C. Upon intramolecular crosslinking, both SCNP-1 and SCNP-2 displayed significantly increased T_g values of 86 °C and 109 °C, respectively. This pronounced increase in T_g can be directly attributed to the progressive increase in intramolecular crosslinking, which effectively restricts segmental motion of the polymer chains. Consequently, T_g increases systematically as the degree of intramolecular crosslinking increases. The higher T_g of SCNP-2 compared to SCNP-1 indicates a more compact and rigid SCNP structure, suggesting that SCNP-2 possesses a higher intramolecular crosslinking. This observation is consistent with literature reports demonstrating that increasing crosslinking density within polymer networks and nanostructures results in elevated T_g values due to constrained molecular dynamics and reduced segmental motion [13,41].

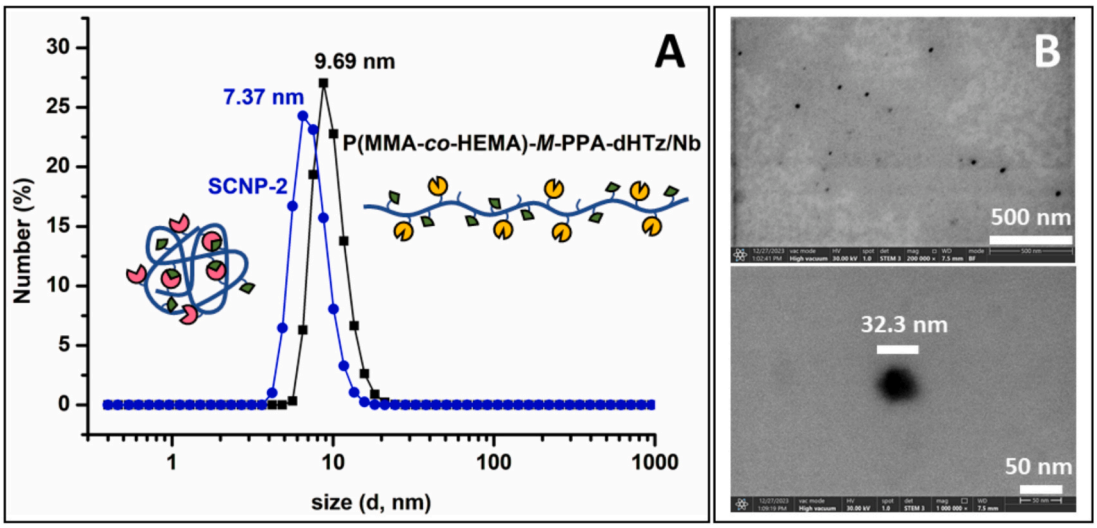

Fig. 8. A) Particle size distirubitions of SCNP-2 (blue) and the precursor polymer (black) by DLS. **B)** STEM images of SCNP-2 at different magnifications.

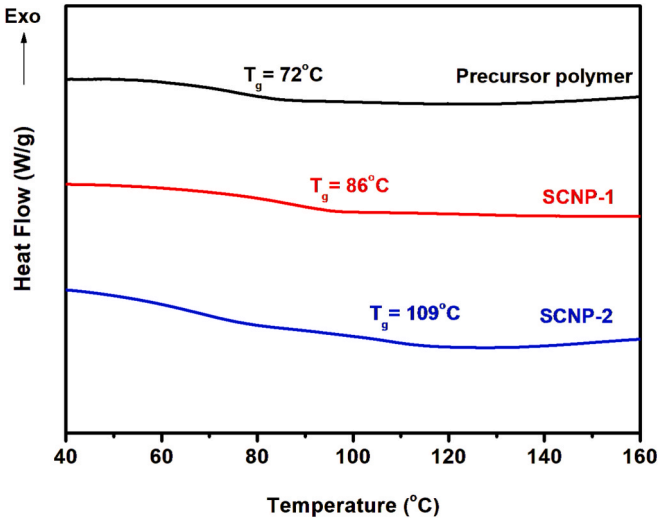

Fig. 9. DSC thermograms of the precursor polymer and SCNPs.

4. Conclusion

Single-chain polymer nanoparticles (SCNPs) have attracted considerable interest for their protein-mimicking folding behavior and their versatility in drug delivery, catalysis, and sensing. In this work, we introduce a novel strategy for SCNP fabrication relying on a photo-induced inverse electron-demand Diels–Alder (photo-IEDDA) reaction. In this approach, the components required for successful intramolecular crosslinking were formed on the same polymer chain. One of these components, namely dihydrotetrazine (dHTz), was kept in inactive form for preventing uncontrolled crosslinking. In the SCNP formation, the dHTz was activated on demand in the reaction medium by photochemical conversion to the reactive tetrazine. Tetrazine derivatives are well-known for their reactivity towards strained olefinic groups and readily undergo conjugation reaction via Diels-Alder reaction. In the work, a P(MMA-co-HEMA), was functionalized with a dHTz derivative and a norbornene derivative through esterification of the HEMA units. UV–Vis spectroscopy analysis showed that red light exposure of the modified polymer, P(MMA-co-HEMA)-M−PPA−dHTz/Nb, in the presence of a photosensitizer led to *in situ* conversion of the dHTz groups to the reactive tetrazines which subsequently underwent intramolecular crosslinking with Nb groups on the same polymer chain. DLS analysis and microscopic images exhibited the resultant SCNPs had less than10 nm size with excellent structural control. By coupling light-triggered activation with the efficiency of click chemistry, this method enables scalable access to well-defined SCNPs with tunable properties, paving the way for advanced applications in nanotechnology and materials science.

CRediT authorship contribution statement

Adalet Nur Altunkaya: Writing – original draft, Visualization, Validation, Methodology, Investigation, Data curation. **Binnur Aydogan Temel:** Writing – review & editing, Methodology, Investigation, Formal analysis, Conceptualization. **Muhammet U. Kahveci:** Writing – original draft, Visualization, Supervision, Resources, Project administration, Investigation, Funding acquisition, Formal analysis, Conceptualization.

Funding

This work was supported by Istanbul Technical University Scientific Research Projects Coordination Unit (ITU-BAP) with grant number PTA-2023–44981.

Declaration of competing interest

The authors declare that they have no known competing financial interests or personal relationships that could have appeared to influence the work reported in this paper.

Appendix A. Supplementary data

Supplementary data to this article can be found online at https://doi.org/10.1016/j.eurpolymj.2026.114509.

Data availability

Data will be made available on request.

References

[1] C.K. Lyon, A. Prasher, A.M. Hanlon, B.T. Tuten, C.A. Tooley, P.G. Frank, E.B. Berda, A brief user's guide to single-chain nanoparticles, Polym. Chem. 6 (2) (2015) 181–197.
[2] H. Frisch, B.T. Tuten, C. Barner-Kowollik, Macromolecular superstructures: a future beyond single chain nanoparticles, Isr. J. Chem. 60 (1–2) (2020) 86–99.

[3] K. Mundsinger, A. Izuagbe, B.T. Tuten, P.W. Roesky, C. Barner-Kowollik, Single chain nanoparticles in catalysis, Angew. Chem. Int. Ed. 63 (7) (2024) e202311734.
[4] Z. Hu, H. Pu, Single-chain polymer nanoparticles carried cuprous catalysts, Eur. Polym. J. 143 (2021) 110194.
[5] M.A.J. Gillissen, I.K. Voets, E.W. Meijer, A.R.A. Palmans, Single chain polymeric nanoparticles as compartmentalised sensors for metal ions, Polym. Chem. 3 (11) (2012) 3166–3174.
[6] W. Fan, X. Tong, F. Farnia, B. Yu, Y. Zhao, CO2-responsive polymer single-chain nanoparticles and self-assembly for gas-tunable nanoreactors, Chem. Mater. 29 (13) (2017) 5693–5701.
[7] A. Latorre-Sanchez, J.A. Pomposo, A simple, fast and highly sensitive colorimetric detection of zein in aqueous ethanol via zein–pyridine–gold interactions, Chem. Commun. 51 (86) (2015) 15736–15738.
[8] C.-C. Cheng, S.-Y. Huang, W.-L. Fan, A.-W. Lee, C.-W. Chiu, D.-J. Lee, J.-Y. Lai, Water-soluble single-chain polymeric nanoparticles for highly selective cancer chemotherapy, ACS Appl. Polym. Mater. 3 (1) (2020) 474–484.
[9] N.M. Hamelmann, J.M.J. Paulusse, Single-chain polymer nanoparticles in biomedical applications, J. Control. Release 356 (2023) 26–42.
[10] P.A. Dykeman-Bermingham, L.R. Stingaciu, C. Do, A.S. Knight, Dynamic implications of noncovalent interactions in amphiphilic single-chain polymer nanoparticles, ACS Macro Lett. 13 (7) (2024) 889–895.
[11] M. Iguaran, S. Gutierrez-Lkourt, E. Verde-Sesto, A. Maestro, J.A. Pomposo, Size conformation, and local domains of single-chain nanoparticles with intrachain covalent, dipolar, and electrostatic interactions: toward artificial intrinsically disordered proteins, Macromolecules 58 (15) (2025) 8536–8554.
[12] S. Gillhuber, J.A. Kammerer, A. Quinn, J.O. Holloway, K. Mundsinger, E. Liarou, D. Golberg, H. Frisch, M.L. O'Mara, C. Barner-Kowollik, P.W. Roesky, Control over Ba(ii)-mediated single-chain polymer nanoparticle compaction by dynamic metal complexation, Polym. Chem. 16 (41) (2025) 4537–4547.
[13] I. Dashan, D.K. Balta, B.A. Temel, G. Temel, Preparation of single chain nanoparticles via photoinduced radical coupling process, Eur. Polym. J. 113 (2019) 183–191.
[14] J. Willenbacher, K.N.R. Wuest, J.O. Mueller, M. Kaupp, H.-A. Wagenknecht, C. Barner-Kowollik, Photochemical design of functional fluorescent single-chain nanoparticles, ACS Macro Lett. 3 (6) (2014) 574–579.
[15] F. Genc, G. Temel, B.A. Temel, Single-chain polymeric nanoparticles using 4-armed star copolymers, Polymer 201 (2020) 122659.
[16] A. Sanchez-Sanchez, A. Arbe, J. Colmenero, J.A. Pomposo, Metallo-folded single-chain nanoparticles with catalytic selectivity, ACS Macro Lett. 3 (5) (2014) 439–443.
[17] A.R. de Luzuriaga, N. Ormategui, H.J. Grande, I. Odriozola, J.A. Pomposo, I. Loinaz, Intramolecular click cycloaddition: an efficient room-temperature route towards bioconjugable polymeric nanoparticles, Macromol. Rapid Commun. 29 (12–13) (2008) 1156–1160.
[18] X. Tian, R. Xue, F. Yang, L. Yin, S. Luan, H. Tang, Single-chain nanoparticle-based coatings with improved bactericidal activity and antifouling properties, Biomacromolecules 22 (10) (2021) 4306–4315.
[19] B. Alkan, B.A. Temel, H. Durmaz, G. Temel, Preparation of poly (oxanorbornene) based single and double-folding polymers via nucleophilic aromatic substitution reaction, Eur. Polym. J. 203 (2024) 112694.
[20] A.P.P. Kröger, R.J.E.A. Boonen, J.M.J. Paulusse, Well-defined single-chain polymer nanoparticles via thiol-Michael addition, Polymer 120 (2017) 119–128.
[21] A.P.P. Kröger, N.M. Hamelmann, A. Juan, S. Lindhoud, J.M.J. Paulusse, Biocompatible single-chain polymer nanoparticles for drug delivery—A dual approach, ACS Appl. Mater. Interfaces 10 (37) (2018) 30946–30951.
[22] B. Alkan, O. Daglar, B.A. Temel, H. Durmaz, G. Temel, Rapid synthesis of polyester based single-chain polymeric nanoparticles via an intra-molecular aza-Michael addition reaction, Polym. Chem. 13 (17) (2022) 2442–2449.
[23] E.J. Foster, E.B. Berda, E.W. Meijer, Metastable supramolecular polymer nanoparticles via intramolecular collapse of single polymer chains, J. Am. Chem. Soc. 131 (20) (2009) 6964–6966.
[24] T. Terashima, T. Mes, T.F.A. De Greef, M.A.J. Gillissen, P. Besenius, A.R. A. Palmans, E.W. Meijer, Single-chain folding of polymers for catalytic systems in water, J. Am. Chem. Soc. 133 (13) (2011) 4742–4745.
[25] M.L. Blackman, M. Royzen, J.M. Fox, Tetrazine ligation: fast bioconjugation based on inverse-electron-demand diels-alder reactivity, J. Am. Chem. Soc. 130 (41) (2008) 13518–13519.
[26] J.A. Prescher, C.R. Bertozzi, Chemistry in living systems, Nat. Chem. Biol. 1 (1) (2005) 13–21.
[27] E.M. Sletten, C.R. Bertozzi, Bioorthogonal chemistry: fishing for selectivity in a sea of functionality, Angewandte Chemie-International Edition 48 (38) (2009) 6974–6998.
[28] D.L. Alge, M.A. Azagarsamy, D.F. Donohue, K.S. Anseth, Synthetically tractable click hydrogels for three-dimensional cell culture formed using tetrazine-norbornene chemistry, Biomacromolecules 14 (4) (2013) 949–953.
[29] O.J. George, J. Song, J.M. Benson, Y. Fang, H. Zhang, D.L. Burris, J.M. Fox, X. Jia, Tunable synthesis of hydrogel microfibers via interfacial tetrazine ligation, Biomacromolecules 23 (7) (2022) 3017–3030.
[30] C.F. Hansell, A. Lu, J.P. Patterson, R.K. O'Reilly, Exploiting the tetrazine–norbornene reaction for single polymer chain collapse, Nanoscale 6 (8) (2014) 4102–4107.
[31] Y. Fu, N.A. Simeth, W. Szymanski, B.L. Feringa, Visible and near-infrared light-induced photoclick reactions, Nat. Rev. Chem. 8 (9) (2024) 665–685.
[32] B.D. Fairbanks, L.J. Macdougall, S. Mavila, J. Sinha, B.E. Kirkpatrick, K.S. Anseth, C.N. Bowman, Photoclick chemistry: a bright idea, Chem. Rev. 121 (12) (2021) 6915–6990.
[33] N. Özbek, E.L. Sahkulubey Kahveci, M.U. Kahveci, Light-induced inverse electron demand diels–alder reaction as an approach for grafting macromolecules to glass surfaces, ACS Appl. Polym. Mater. 3 (8) (2021) 3721–3732.
[34] V.X. Truong, K.M. Tsang, F. Ercole, J.S. Forsythe, Red light activation of tetrazine–norbornene conjugation for bioorthogonal polymer cross-linking across tissue, Chem. Mater. 29 (8) (2017) 3678–3685.
[35] H. Zhang, W.S. Trout, S. Liu, G.A. Andrade, D.A. Hudson, S.L. Scinto, K.T. Dicker, Y. Li, N. Lazouski, J. Rosenthal, C. Thorpe, X. Jia, J.M. Fox, Rapid bioorthogonal chemistry turn-on through enzymatic or long wavelength photocatalytic activation of tetrazine ligation, J. Am. Chem. Soc. 138 (18) (2016) 5978–5983.
[36] Z.M. Png, H. Zeng, Q. Ye, J. Xu, Inverse-electron-demand diels–alder reactions: principles and applications, Chemistry–an Asian Journal 12 (17) (2017) 2142–2159.
[37] H. Zhang, W.S. Trout, S. Liu, G.A. Andrade, D.A. Hudson, S.L. Scinto, K.T. Dicker, Y. Li, N. Lazouski, J. Rosenthal, Rapid bioorthogonal chemistry turn-on through enzymatic or long wavelength photocatalytic activation of tetrazine ligation, J. Am. Chem. Soc. 138 (18) (2016) 5978–5983.
[38] M.R. Islam, L.G. Bach, J.M. Park, S.S. Hong, K.T. Lim, Synthesis and characterization of poly (HEMA-co-MMA)-g-POSS nanocomposites by combination of reversible addition fragmentation chain transfer polymerization and click chemistry, J. Appl. Polym. Sci. 127 (3) (2013) 1569–1577.
[39] C. Wang, H. Zhang, T. Zhang, X. Zou, H. Wang, J.E. Rosenberger, R. Vannam, W. S. Trout, J.B. Grimm, L.D. Lavis, C. Thorpe, X. Jia, Z. Li, J.M. Fox, Enabling in vivo photocatalytic activation of rapid bioorthogonal chemistry by repurposing silicon-rhodamine fluorophores as cytocompatible far-red photocatalysts, J. Am. Chem. Soc. 143 (28) (2021) 10793–10803.
[40] D. Mecerreyes, V. Lee, C.J. Hawker, J.L. Hedrick, A. Wursch, W. Volksen, T. Magbitang, E. Huang, R.D. Miller, A novel approach to functionalized nanoparticles: self-crosslinking of macromolecules in ultradilute solution, Adv. Mater. 13 (3) (2001) 204–208.
[41] B. Alkan, B.A. Temel, H. Durmaz, G. Temel, Preparation of poly(oxanorbornene) based single and double-folding polymers via nucleophilic aromatic substitution reaction, Eur. Polym. J. 203 (2024) 112694.